Journal of Fluids and Structures (2002) **16**(1), 93–112
doi:10.1006/jfls.2001.0411, available online at http://www.idealibrary.com on IDEAL®

FLUIDELASTIC ANALYSIS OF TUBE BUNDLE VIBRATION IN CROSS-FLOW

H. TANAKA, K. TANAKA AND F. SHIMIZU

Department of Mechanical System Engineering, Kyushu Institute of Technology 640-4 Kawazu Iizuka-City, Fukuoka Prefecture, 820-8502, Japan

AND

S. TAKAHARA

Ryoken Tech. Co. Ltd., Nagasaki, Japan

(Received 1 September 2000, and in final form 15 May 2001)

Tube bundles in cross-flow vibrate in response to motion-induced fluid-dynamic forces; hence, the resultant motions are considered to be a fluidelastic vibration. The characteristics of the vibration depend greatly on the features of the fluid-dynamic forces and the structure of the tube bundle. Therefore, in this study, the equations of motion of the tube bundle are derived. From the viewpoint of vibration, each tube is not independent of the surrounding tubes because its vibration is affected by fluid-dynamic coupling with the neighboring tubes. Thus, the equations are a set of coupled equations and the solution is obtained as an eigenvalue problem. The fluid-dynamic forces, which are indispensable in the calculation, have been obtained by experiments using a vibrating tube in the bundle; it was found that the forces depend strongly on the reduced velocity. Using these equations and the fluid forces, critical velocities of the tube bundle vibration are calculated, and it is found that the critical velocity is strongly dependent on the fluid-dynamic force characteristics, as they vary with the reduced velocity. Vibration tests of the tube bundle have also been conducted, and the critical velocities obtained in the tests are compared with the calculated values; agreement with the calculated values is good, demonstrating that the method of calculation is useful. The effects of mass ratio, frequency deviation and damping deviation of tubes in the bundle on the critical velocity are also examined theoretically. It is found that it is better to treat the mass ratio and the logarithmic decrement separately when the mass ratio is less than 10. Differences in natural frequencies make the critical velocity large. Similarly, differences in logarithmic decrement may distribute the vibration energy to other tubes and make the critical velocity large.

1. INTRODUCTION

IT IS WELL KNOWN THAT A TUBE BUNDLE of a heat exchanger in cross-flow sometimes vibrates. Much research has been carried out on the problem over the past quarter-century, and many things have been found. These researches have been discussed in detail in the literature (Paidoussis 1983; Weaver & Fiztpatrick 1988; Price 1995). Price reviewed the papers and classified the theoretical models for tube-bundle vibration as follows: jet switch models, quasi-static models, inviscid flow models: unsteady models, semi-analytical models, quasi-steady models, and computational fluid-dynamic models.

The details of each model are given in the literature. However, Price states that the "unsteady model" is the most reliable one. The unsteady model is a method of calculation using unsteady fluid-dynamic forces that act on the vibrating tube bundle. This may

0889–9746/02/010093 + 20 $35.00/0

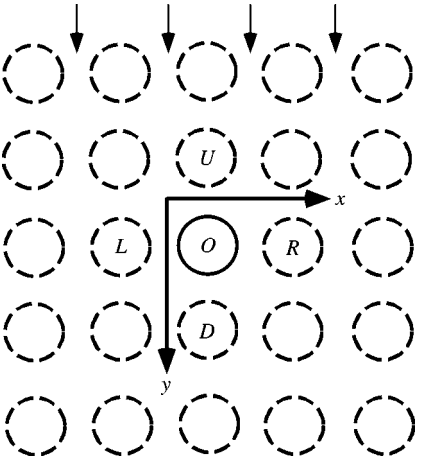

Figure 1. Tube arrangement.

physically be the most accurate model because the directly measured fluid forces are used. In order to clarify the problems of tube vibration in cross-flow, an analysis of the unsteady model was carried out using the unsteady fluid-dynamic forces that were presented earlier by Tanaka & Takahara (1980, 1981).

2. THEORY

2.1. Expression of Fluid Dynamic Force Acting on Tube Bundle

The tube bundle in a square array shown in Figure 1 was used in this study. Pitch-to-diameter ratio is 1.33. The characteristics of the fluid-dynamic forces are discussed in Tanaka & Takahara (1980, 1981), so only a brief explanation is given here. The fluid-dynamic force that acts on a tube (O) in Figure 1 must be a function of the tubes (O, L, R, U, D) vibrating in the x- and y-directions.

If the fluid-dynamic forces are linear and superposable, the equations may be expressed as follows:

$$F_x = \frac{1}{2}\rho U^2 \sum_{k=1}^{5} (c_{xkx} X_k + c_{xky} Y_k), \tag{1}$$

$$F_y = \frac{1}{2}\rho U^2 \sum_{k=1}^{5} (c_{ykx} X_k + c_{yky} Y_k). \tag{2}$$

Here, $k = 1$–5 corresponds to the tubes (O, L, R, U, D), and X and Y denote the vibration displacements in the x- and y-direction, respectively. Each fluid-dynamic force coefficient is identified by three suffixes. The first suffix is associated with the direction of the fluid force, the second with the position of the vibrating tube and the third with the direction of tube vibration. For example, c_{xLy} is the coefficient for the fluid-dynamic force on tube (O) in the x-direction induced by the tube (L) vibrating in the y-direction. In the case of a square array, the following relations are obtained from the geometrical properties of the array:

$$c_{xRx} = c_{xLx},\ c_{yRy} = c_{yLy},\ c_{xRy} = -c_{xLy},\ c_{yRx} = -c_{yLx},$$

$$c_{xOy} = c_{yOx} = c_{xUy} = c_{yUx} = c_{xDy} = c_{yDx} = 0.$$

Using these relations, equation (1) and (2) may be expressed as follows:

$$F_x = \frac{1}{2}\rho U^2 \{c_{xOx} X_O + c_{xLx}(X_L + X_R) + c_{xLy}(Y_L - Y_R) + c_{xUx} X_U + c_{xDx} X_D\}, \quad (3)$$

$$F_y = \frac{1}{2}\rho U^2 \{c_{yOy} Y_O + c_{yLx}(X_L - X_R) + c_{yLy}(Y_L + Y_R) + c_{yUy} Y_U + c_{yDy} Y_D\}. \quad (4)$$

The vibration of the tube is assumed to be harmonic. Hence, the amplitude is expressed as

$$X = X_0 \cos(\omega t). \quad (5)$$

Using this equation, the force acting on the tube may be written as follows:

$$\begin{aligned} F &= \frac{\pi\rho d^2}{4} c_m \ddot{X} + \frac{1}{2}\rho d U c_d \dot{X} + \frac{1}{2}\rho U^2 c_k X \\ &= \frac{1}{2}\rho U^2 X_0 \left\{ \left(\frac{-2\pi^3}{V_r^2} c_m + c_k \right) \cos(\omega t) - \frac{2\pi}{V_r} c_d \sin(\omega t) \right\}, \end{aligned} \quad (6)$$

where c_m is the added mass coefficient, c_d is the damping coefficient, c_k is the stiffness coefficient and V_r is the reduced velocity defined by

$$V_r = \frac{2\pi U}{\omega d}.$$

Equation (6) may be re-written in terms of an amplitude c_o and phase difference φ as follows:

$$F = -\frac{1}{2}\rho U^2 X_0 c_0 \cos(\omega t + \varphi). \quad (7)$$

However, the amplitude c_o and the phase φ are functions of the reduced velocity V_r. The negative symbol has been introduced on the right-hand side of equation (7), because the direction in which the force works and the direction of the vibration displacement are opposite to each other.

In the case of the unsteady model, it is reasonable to decompose the fluid-dynamic force into three components: inertia force proportional to acceleration, the damping force proportional to velocity and the stiffness force proportional to the displacement. As the inertia force is not dependent on the flow velocity, the added mass is obtained easily by a simple experiment or a calculation with potential flow theory in still water. On the other hand, it is very difficult to obtain the damping and stiffness forces. Nevertheless, if the amplitudes and phase differences of the fluid-dynamic forces at each reduced velocity are obtained, it becomes possible to obtain damping and stiffness forces from equation (6) and (7) as follows:

$$c_m = \text{known value}, \quad (8)$$

$$c_d = -\frac{V_r}{2\pi} c_o \sin\varphi, \qquad c_k = -c_o \cos\varphi + \frac{2\pi^3}{V_r^2} c_m. \quad (9, 10)$$

2.2. Equation of Motion

The structural forces are considered first. It is assumed that the mass of a tube is uniformly distributed and that the tube vibrates with vibration mode ξ that is a function of z. The number of tubes constituting the bundle is considered to be N. The number of degrees of

freedom is $2N$, because each tube has two degrees of freedom, one in the x- and the other in the y-directions. The fluid-dynamic force depends on the mode shape for each mode $i(1 \leq i \leq 2N)$, so they are identified using the suffix i. Here, superscript s is also added on the top in order to clarify it as the structural force. Therefore, we define the equivalent mass of the tube as

$$m_i^s = \int_0^z m\xi_i^2 \, \mathrm{d}z, \tag{11}$$

the equivalent damping coefficient

$$D_i^s = m_i^s \frac{\delta_i^s}{\pi} \omega_i \tag{12}$$

and the equivalent stiffness

$$k_i^s = m_i^s \omega_i^2, \tag{13}$$

where m, δ_i^s and ω_i are the tube mass per unit length, the logarithmic decrement, and the angular frequency, respectively.

Next, the fluid-dynamic force is considered. The index j is similarly introduced to identify the vibrating tube that generates the fluid-dynamic force. Let us discuss the fluid-dynamic force on vibrating tube i induced by the vibration of tube j. In the case where the flow is not uniform along z-axis, each coefficient is expressed as follows:

$$\text{mass: } m_{ij}^f = \frac{\pi\rho d^2}{4} \int_0^z c_{mij}\xi_i\xi_j \, \mathrm{d}z, \tag{14}$$

$$\text{damping: } D_{ij}^f = \frac{\rho dU}{2} \int_0^z c_{dij}\eta\xi_i\xi_j \, \mathrm{d}z, \tag{15}$$

$$\text{stiffness: } k_{ij}^f = \frac{\rho U^2}{2} \int_0^z c_{kij}\eta^2\xi_i\xi_j \, \mathrm{d}z. \tag{16}$$

Superscript f stands for the fluid-dynamic force.

The following nondimensional equivalent values are introduced next:

$$\mu_i = m_i^s \Big/ \left(\rho d^2 \int_0^z \xi_i^2 \, \mathrm{d}z\right), \quad C_{mij}^f = \int_0^z c_{mij}\xi_i\xi_j \, \mathrm{d}z \Big/ \int_0^z \xi_i^2 \, \mathrm{d}z,$$

$$C_{dij}^f = \int_0^z c_{dij}\eta\xi_i\xi_j \mathrm{d}z \Big/ \int_0^z \xi_i^2 \, \mathrm{d}z, \quad C_{kij}^f = \int_0^z c_{kij}\eta^2\xi_i\xi_j \mathrm{d}z \Big/ \int_0^z \xi_i^2 \, \mathrm{d}z.$$

By combining the structural forces and fluid-dynamic forces in each term, the following matrices are obtained using the above nondimensional equivalent values:

elements of mass matrix

$$m_{ij} = m_i^s + m_{ij}^f = m_i^s \left(\delta_{cij} + \frac{\pi C_{mij}^f}{4\mu_i}\right), \tag{17}$$

elements of damping matrix

$$D_{ij} = D_i^s + D_{ij}^f = m_i^s \left(\frac{\omega_i \delta_i^s}{\pi} \delta_{cij} + \frac{C_{dij}^f U}{2\mu_i d}\right), \tag{18}$$

elements of stiffness matrix

$$k_{ij} = k_i^s + k_{ij}^f = m_i^s\left(\omega_i^2\delta_{cij} + \frac{C_{kij}^f U^2}{2\mu_i d^2}\right), \tag{19}$$

where δ_{cij} is Kronecker's delta, equal to 1 for $i = j$, and otherwise equal to zero.

So, the equation of motion of tube i is expressed as follows:

$$\sum_{j=1}^{2N}(m_{ij}\ddot{X}_j + D_{ij}\dot{X}_j + k_{ij}X_j) = 0. \tag{20}$$

Let us now introduce a nondimensional form of equation (20). Using the frequency ω and the tube diameter d for nondimensionalization, we introduce

$$\tau = t\omega, \quad X^* = X/d, \quad \dot{X}^* = \partial X^*/\partial\tau = \dot{X}/\mathrm{d}\omega, \quad \ddot{X}^* = \partial^2 X^*/\partial\tau^2 = \ddot{X}/\mathrm{d}\omega^2,$$

where the amplitude X^* and time τ are nondimensional.

Each tube vibration has its own natural frequency ω_i. The ratio of the natural frequency ω_i and the reference frequency ω_o is defined as the frequency ratio,

$$\Omega_i = \omega_i/\omega_o.$$

The real frequency ω at which the tube bundle vibrates in fluid flow is not always equal to the reference frequency ω_0 or to the natural frequency ω_i, because the fluid-dynamic forces change the frequency. It is impossible to know the frequency ω beforehand, so the predictive value λ_{Ia} is introduced:

$$\lambda_{Ia} = \omega/\omega_o.$$

Substituting equations (17), (18) and (19) into equation (20) and introducing the terms Ω_i and λ_{Ia} defined above, the following nondimensional equation is obtained:

$$\sum_{j=1}^{2N}\left\{\left(\delta_{cij} + \frac{\pi}{4}\frac{C_{mij}^f}{\mu_i}\right)\ddot{X}_j^* + \left(\frac{\delta_i^s\Omega_i}{\pi\lambda_{Ia}}\delta_{cij} + \frac{1}{4\pi}\frac{C_{dij}^f}{\mu_i}V_r\right)\dot{X}_j^* + \left(\frac{\Omega_i^2}{\lambda_{Ia}^2}\delta_{cij} + \frac{1}{8\pi^2}\frac{C_{kij}^f}{\mu_i}V_r^2\right)X_j^*\right\} = 0. \tag{21}$$

This is a set of coupled equations of motion in dimensionless form and gives rise to a second-order eigenvalue problem. The inertia force coefficient, damping coefficient and stiffness coefficient of each fluid-dynamic force can be calculated with equations (8)–(10). In addition, the fluid-dynamic forces corresponding to the suffixes i and j are obtained with equations (3) and (4).

Equation (21) consists of the equations of motion of each tube, so it is possible to apply this equation to tube bundles having various and complicated structural conditions. For example, the tube bundles having different characteristics for each individual tube, such as different natural frequencies, different masses, different vibration modes and different damping ratios, can be considered.

2.3. Calculation Procedure

At first, it is necessary to assume a value for the reduced velocity, because the unsteady fluid-dynamic force is a function of reduced velocity. Next, the predictive value λ_{Ia} must be assumed. Since the frequency ω in which the tube bundle will actually vibrate is not known, it is convenient to assume that λ_{Ia} is equal to unity. By substituting these values into

equation (21), the eigenvalues are obtained. The eigenvalues are generally complex, i.e.

$$\lambda = \lambda_R + \mathrm{i}\lambda_I.$$

Then, the vibration is expressed as follows:

$$X = X_o e^{\lambda t} = X_o \mathrm{e}^{(\lambda_R + \mathrm{i}\lambda_I)t}.$$

The real part of the eigenvalue indicates the rate of increase or decrease of the vibration amplitude with time, and the imaginary part is the frequency.

The vibration of the tube bundle has many degrees of freedom, and hence many eigenvalues are obtained. However, the most susceptible vibration mode is that having the largest value of the real part λ_R. The imaginary part λ_I shows the ratio between the reference frequency ω_o and the frequency ω in which the tube bundle actually vibrates.

If the calculated frequency λ_I differs more than a little from the estimated value λ_{Ia}, the estimated value must be replaced by the calculated value as follows:

$$\lambda_{Ia} \neq \lambda_I \rightarrow \lambda_{Ia} = \lambda_I.$$

The calculation must be repeated until the calculated value agrees with the estimated value.

The logarithmic decrement can be expressed as follows:

$$\delta = -2\pi\lambda_R.$$

If the structural damping is assumed to be zero at first, the logarithmic decrement that is required to quench the vibration is expressed as

$$\delta_c = 2\pi\lambda_R. \tag{22}$$

The reduced velocity based on the reference frequency is as follows:

$$V_{ro} = V_r \lambda_I. \tag{23}$$

3. VERIFICATION OF THE THEORY

3.1. Data of Fluid-Dynamic Force

The unsteady fluid-dynamic forces used in this analysis were determined from the same data that were used previously (Tanaka & Takahara 1980, 1981). There are two types of tube arrangements. One is a square array with a pitch-to-diameter ratio of 1·33, and the other is a single row of tubes with a pitch-to-diameter ratio of 1·33. The fluid-dynamic forces consist of the fluid-dynamic force coefficients and phase differences as in equation (7). Added mass coefficients are also necessary. The fluid-dynamic coefficients are listed in Tables 1 and 2. The first row in each table shows the inertia force coefficients due to added mass, and the other rows show the fluid-dynamic force coefficients and phase differences at each reduced velocity.

3.2. Result of Calculation

It is first assumed that the tube characteristics (mass, natural frequency, logarithmic decrement) of all tubes are equal, in order to simplify the problem. Under such conditions, the structural characteristics that affect the critical velocity are only the mass ratio μ and the logarithmic decrement δ, as equation (21) shows. So, the effects of mass ratio and logarithmic decrement on the critical velocity were examined.

TABLE 1
Fluid-dynamic forces in a square tube array with a pitch to diameter ratio of 1·33

V_r		C_{xLx}	C_{xLy}	C_{yLx}	C_{yLy}	C_{xOx}	C_{yOy}	C_{xUx}	C_{xDx}	C_{yUy}	C_{yDy}
0	C_m	− 0·29	0·0	0·0	0·33	1·28	1·28	0·33	0·33	− 0·29	− 0·29
1·5	C_0	10·5	5·2	1·9	10·5	39·0	38·0	10·8	10·8	8·0	9·5
	ϕ	− 174	100	101	1	− 3	− 3	5	− 6	− 172	175
2·0	C_0	6·00	3·50	2·60	5·90	21·00	21·50	6·00	4·20	4·60	5·20
	ϕ	− 171	106	68	2	− 3·3	− 6	10	− 15	− 169	174
2·5	C_0	4·00	2·90	2·70	3·00	14·00	12·50	4·05	2·60	3·10	3·00
	ϕ	− 165	116	70	5	− 7	− 13	15	− 25	− 165	172
3·0	C_0	2·80	2·40	2·40	1·30	9·80	7·50	2·65	2·10	1·95	1·60
	ϕ	− 158	130	72	8	− 4·1	− 23	24	− 32	− 157	149
3·5	C_0	2·00	2·05	2·00	0·70	6·60	4·70	1·90	1·80	0·90	0·95
	ϕ	− 146	144	70	− 50	0	− 32	33	− 42	− 120	137
4·0	C_0	1·40	1·75	1·80	1·00	5·00	3·80	1·45	1·65	0·33	0·82
	ϕ	− 128	156	68	− 83	1·4	− 44	42	− 54	− 30	128
5·0	C_0	0·95	1·20	1·50	1·20	2·90	3·00	0·90	1·40	0·61	0·79
	ϕ	− 104	176	66	− 82	4	− 51	53	− 76	90	116
6·0	C_0	0·82	0·86	1·37	1·03	1·90	2·55	0·60	1·28	0·69	0·73
	ϕ	− 85	− 169	60	− 74	9	− 54	56	− 94	100	102
7·0	C_0	0·77	0·64	1·28	0·90	1·25	2·20	0·46	1·25	0·46	0·67
	ϕ	− 66	− 155	56	− 70	15	− 55	51	− 104	107	90
8·0	C_0	0·72	0·46	1·22	0·80	0·85	1·95	0·36	1·25	0·31	0·57
	ϕ	− 49	− 143	52	− 70	22	− 57	35	− 107	112	83
10·0	C_0	0·63	0·30	1·12	0·69	0·39	1·55	0·27	1·25	0·24	0·47
	ϕ	− 15	− 124	50	− 70	60	− 60	11	− 110	− 116	79
12·0	C_0	0·55	0·25	1·05	0·66	0·28	1·25	0·23	1·05	0·21	0·45
	ϕ	2	− 110	50	− 70	138	− 62	− 5	− 110	119	80
15·0	C_0	0·50	0·22	0·99	0·64	0·60	1·00	0·21	0·87	0·17	0·44
	ϕ	10	− 96	49	− 76	160	− 66	− 22	− 110	122	83
20·0	C_0	0·46	0·21	0·90	0·62	0·81	0·82	0·19	0·69	0·16	0·39
	ϕ	15	− 72	48	− 82	162	− 70	− 40	− 105	128	92
25·0	C_0	0·45	0·23	0·81	0·60	0·94	0·70	0·21	0·59	0·15	0·36
	ϕ	12	− 64	48	− 78	161	− 70	− 42	− 96	132	100
30·0	C_0	0·45	0·24	0·73	0·60	1·00	0·65	0·24	0·53	0·15	0·32
	ϕ	10	− 53	48	− 69	159	− 64	− 42	− 87	137	109
35·0	C_0	0·44	0·26	0·67	0·60	1·05	0·60	0·27	0·50	0·15	0·30
	ϕ	16	− 44	47	− 56	158	− 58	− 40	− 80	140	115
40·0	C_0	0·44	0·27	0·62	0·60	1·08	0·56	0·30	0·51	0·15	0·27
	ϕ	25	− 36	47	− 42	157	− 52	− 39	− 75	143	123
50·0	C_0	0·45	0·29	0·56	0·59	1·10	0·50	0·34	0·53	0·15	0·24
	ϕ	35	− 24	46	− 32	157	− 42	− 36	− 68	148	133
60·0	C_0	0·45	0·32	0·52	0·59	1·10	0·47	0·36	0·56	0·15	0·21
	ϕ	45	− 14	46	− 32	158	− 36	− 31	− 62	152	141
80·0	C_0	0·45	0·36	0·48	0·59	1·11	0·40	0·36	0·58	0·15	0·17
	ϕ	60	3	46	− 37	161	− 27	− 24	− 56	157	158
100·0	C_0	0·42	0·41	0·46	0·59	1·12	0·37	0·37	0·60	0·15	0·14
	ϕ	72	17	47	− 40	164	− 20	− 20	− 52	162	162

The calculated critical velocities of a square tube array (3 rows, 4 columns) of pitch-to-diameter ratio 1·33 are shown in Figure 2 as a function of mass ratio. The ordinate is the critical reduced velocity, and the abscissa is the logarithmic decrement. The critical velocities of a single row of tubes are shown in Figure 3. The critical velocities in both cases vary in a complicated way with the logarithmic decrement. In particular, the line of critical velocity of the single row array is divided into two regions.

TABLE 2
Fluid-dynamic forces on a single row of tubes with a pitch to diameter ratio of 1·33

V_r		C_{xLx}	C_{xLy}	C_{yLx}	C_{yLy}	C_{xOx}	C_{yOy}
0	C_m	− 0·28	0·0	0·0	0·31	1·11	1·11
1·5	C_0	10·0	4·2	2·0	10·8	29·0	29·0
	ϕ	− 178	95	128	0	0	− 2
2·0	C_0	5·40	2·65	1·28	6·10	17·00	17·00
	ϕ	− 178	116	109	− 3	0	− 2
2·5	C_0	3·50	2·55	0·84	3·90	11·20	9·50
	ϕ	− 174	131	91	− 10	2	− 6
3·0	C_0	2·50	2·25	0·72	2·75	8·00	5·80
	ϕ	− 167	143	73	− 21	5	− 11
3·5	C_0	1·92	1·85	0·78	2·12	6·00	4·10
	ϕ	− 156	154	65	− 34	13	− 19
4·0	C_0	1·55	1·50	0·83	1·72	4·70	3·10
	ϕ	− 140	163	65	− 40	23	− 26
5·0	C_0	1·12	0·97	0·84	1·27	2·90	2·15
	ϕ	− 75	180	72	− 45	60	− 30
6·0	C_0	0·89	0·64	0·77	1·00	2·00	1·72
	ϕ	− 33	− 166	80	− 45	97	− 33
7·0	C_0	0·73	0·44	0·67	0·83	1·60	1·53
	ϕ	− 10	− 152	86	− 45	125	− 38
8·0	C_0	0·63	0·33	0·55	0·70	1·36	1·37
	ϕ	3	− 132	89	− 45	149	− 43
10·0	C_0	0·52	0·22	0·41	0·54	1·13	1·06
	ϕ	17	− 69	92	− 44	188	− 53
12·0	C_0	0·47	0·19	0·34	0·45	1·00	0·81
	ϕ	23	− 45	91	− 44	201	− 59
15·0	C_0	0·43	0·23	0·27	0·37	0·89	0·55
	ϕ	28	− 32	82	− 43	209	− 61
20·0	C_0	0·38	0·33	0·22	0·31	0·78	0·33
	ϕ	30	− 20	36	− 32	217	− 62
25·0	C_0	0·35	0·40	0·18	0·28	0·70	0·26
	ϕ	31	− 15	29	− 17	219	− 60
30·0	C_0	0·33	0·43	0·17	0·27	0·65	0·24
	ϕ	32	− 12	26	− 12	219	− 59
35·0	C_0	0·31	0·47	0·16	0·27	0·60	0·23
	ϕ	32	− 10	25	− 9	218	− 57
40·0	C_0	0·30	0·49	0·15	0·26	0·57	0·23
	ϕ	32	− 9	24	− 7	217	− 55
50·0	C_0	0·28	0·53	0·14	0·26	0·53	0·23
	ϕ	32	− 8	22	− 6	216	− 52
60·0	C_0	0·26	0·56	0·13	0·26	0·49	0·23
	ϕ	31	− 7	20	− 5	215	− 51
80·0	C_0	0·24	0·61	0·12	0·26	0·45	0·22
	ϕ	30	− 6	18	− 3	214	− 50
100·0	C_0	0·23	0·63	0·11	0·26	0·43	0·22
	ϕ	28	− 6	17	− 2	214	− 49

3.3. COMPARISON WITH VIBRATION TESTS

Vibration tests were conducted to elucidate the mechanism of fluidelastic instability. The tubes were supported with elastic spars to vibrate in the x- and y-direction as shown in Figure 4. The mass ratio of the tubes was changed by using solid and hollow cylinders. The logarithmic decrement was varied by changing the material of the spars, using steel, nylon

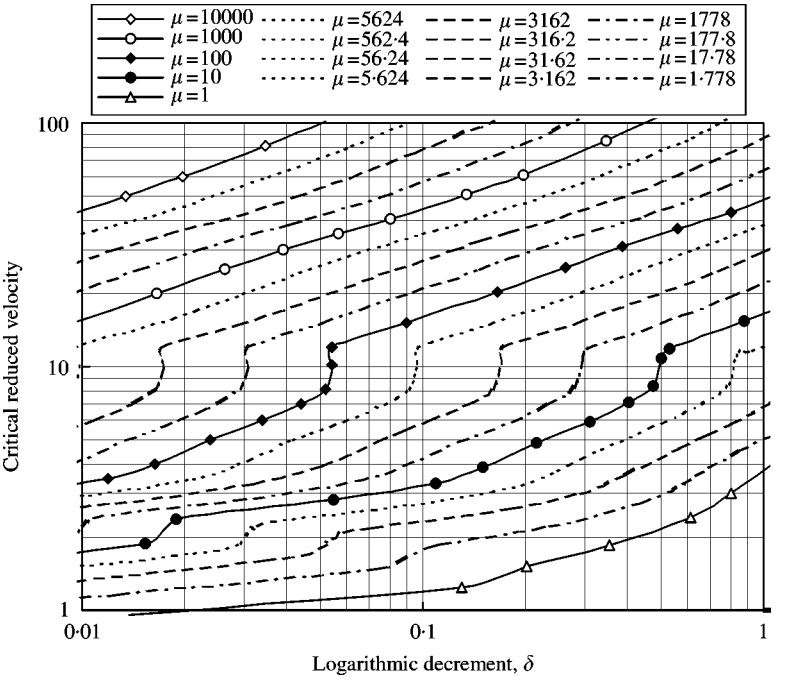

Figure 2. Critical reduced flow velocity for a square tube array versus logarithmic decrement (pitch ratio = 1·33).

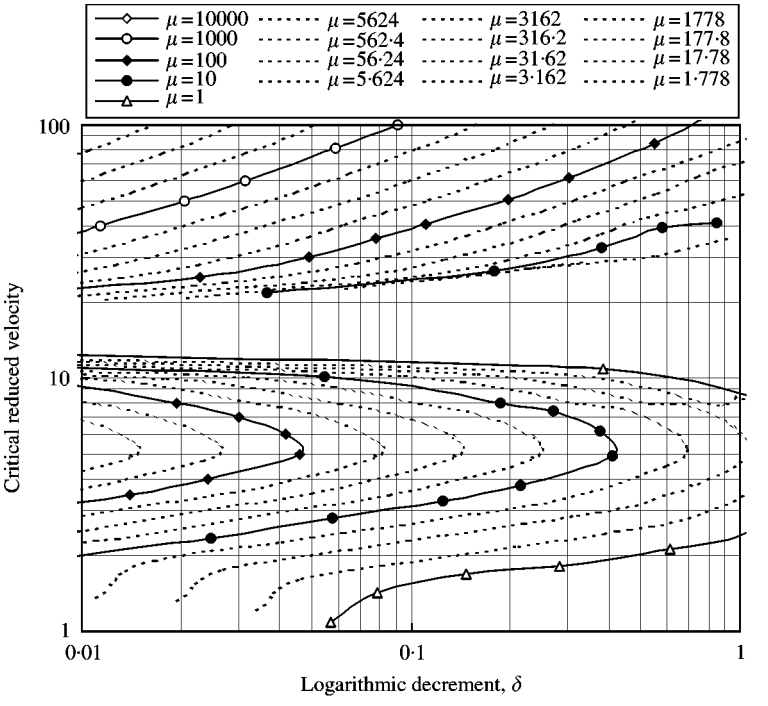

Figure 3. Critical reduced flow velocity for a single row of tubes versus logarithmic decrement (pitch ratio = 1·33).

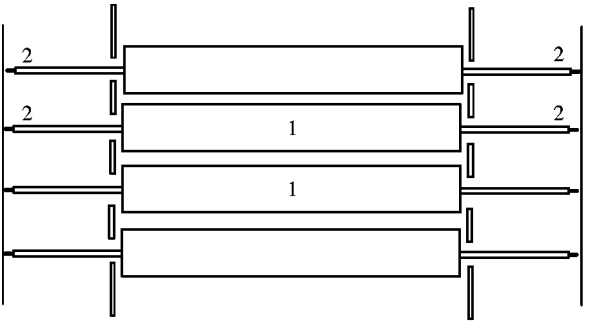

Figure 4. Tube supports for the vibration test. The tubes were 0·3 m long, $d = 0{\cdot}03$ m. 1: rigid tube; 2: elastic struts to allow the tube to vibrate in the x- and y-directions.

TABLE 3
Vibration tests on square tube array (in air flow)

Mass ratio, μ	Logarithmic decrement, δ	Mass damping parameter, $\mu\delta$	Critical velocity, V_r
592·6	0·0045	2·67	12·8
1481	0·0040	5·92	14
1481	0·0061	9·03	14·5
592·6	0·0340	20·1	22
1481	0·0231	34·2	32
1481	0·0314	46·5	36
4444	0·0162	72·0	54
1481	0·0870	129·0	56

TABLE 4
Vibration tests on square tube array (in water flow)

Mass ratio, μ	Logarithmic decrement, δ	Mass damping parameter, $\mu\delta$	Critical velocity, V_r
1·852	0·0023	0·00426	1·35
1·852	0·0061	0·0113	1·45
1·852	0·0297	0·0550	1·75
1·852	0·033	0·0611	1·8
1·852	0·087	0·1611	2·35
1·852	0·166	0·3074	2·7

or acrylic resin. The experiment was conducted in air and in water. The test conditions and test results are shown in Tables 3–5.

Figures 5 and 6 show the critical velocities obtained by calculation and experiment. The experimental data are in good agreement with the calculations, except for a few points but the general characteristics are almost the same. The results show that the unsteady model is able to estimate the critical velocity well.

TABLE 5
Vibration tests on a single row of tubes (in air flow)

Mass ratio, μ	Logarithmic decrement, δ	Mass damping parameter, $\mu\delta$	Critical velocity, V_r
1481·5	0·004	5·92	40
1481·5	0·006	8·89	41
592·6	0·023	13·6	44·5
4444	0·004	17·8	47·5
1481·5	0·028	41·5	68
1481·5	0·04	59·3	89
592·6	0·173	103·0	91
4444	0·031	137·8	125

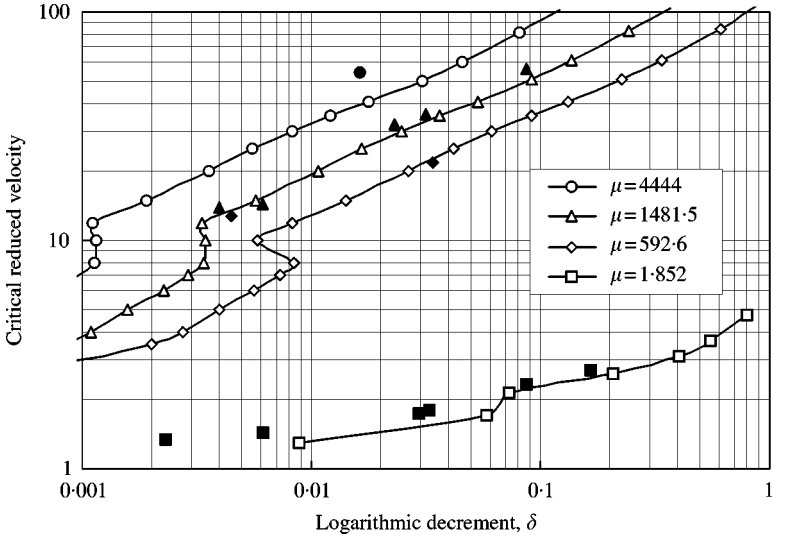

Figure 5. Calculated and experimental critical velocities of the square tube array; dark (filled) symbols are experimental data points.

4. PARAMETRIC STUDY

4.1. EFFECT OF MASS RATIO ON CRITICAL VELOCITY

In most of the researches on tube bundle vibration, the mass-damping parameter $\mu\delta$ is used as a standard variable. However, the mass ratio μ and logarithmic decrement δ are each a fundamentally independent parameter. So, it is necessary to examine as to how far we can apply the combined mass-damping parameter to the estimation of the critical flow velocity. The calculated reduced velocities were rearranged as a function of the mass-damping parameter to get an answer to this question.

The critical velocity of the square tube array with a pitch ratio of 1·33 is shown in Figure 7. If the critical velocity is accurately a function of the mass-damping parameter only, the lines of each mass ratio must be superimposed, giving only one line. When the mass ratio is over 10, the critical velocities are located on almost the same line. This means that the mass ratio has no important effect on the critical velocity. In the case of small mass ratios (less

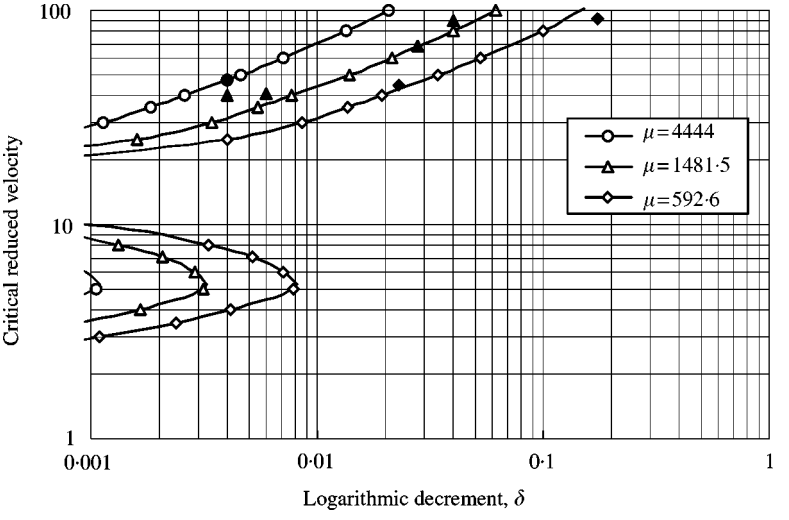

Figure 6. Calculated and experimental critical velocities of a single row of tubes; dark (filled) symbols are experimental data points.

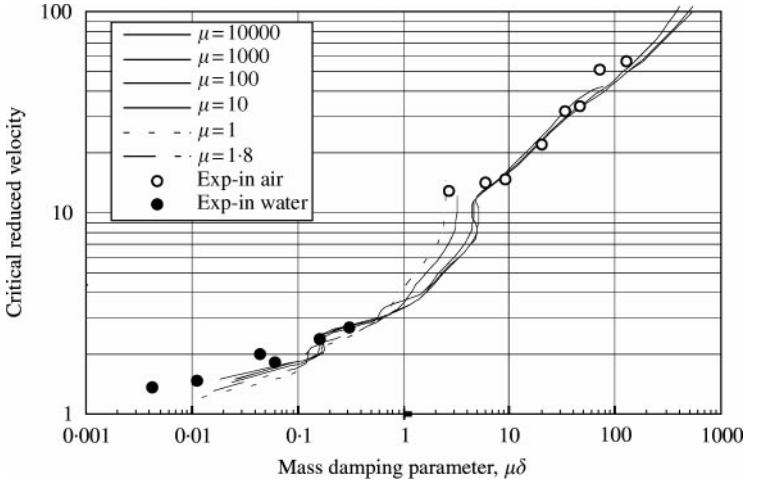

Figure 7. Critical velocity of square tube array versus mass-damping parameter.

than 10), however, the lines are a little different from each other. The critical velocity of mass ratio 1·0 becomes 1·5 to 2·0 times greater in the mass-damping parameter range of 1–5. In the case of a mass ratio of 1·8, the critical velocity gets closer to that of large mass ratio. Experimental data are shown in the figure.

Critical velocities of a single row of tubes are shown in Figure 8. The critical velocities for large mass ratios can be put on the same line, but the velocities for small mass ratios are on different lines, in a similar way as for the square tube array. Experimentally obtained critical velocities are also shown. In this case, the experiment was conducted in air only. It is considered that the critical velocities of tube bundles having a mass ratio less than 10 cannot be treated as if they were a function of the combined mass-damping parameter only.

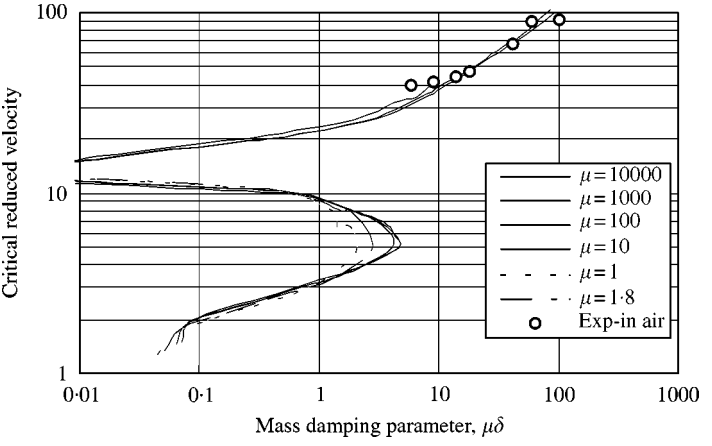

Figure 8. Critical velocity of a single row of tubes versus mass-damping parameter.

4.2. Effect of Stiffness Term and Damping Term

Chen (1983, 1998) showed that fluidelastic vibrations are of two distinct categories. One is associated with the fluid-damping-controlled instability and the other with the fluid-elastic-stiffness-controlled instability. To study this further, the effects of the stiffness and damping terms of the fluid-dynamic force on the critical velocity were examined. Three kinds of calculations were conducted using the unsteady fluid-dynamic forces. The first is the calculation of critical velocity induced only by the damping term of the fluid-dynamic force, the second is that induced by the stiffness term only, and the third is a combined instability that is induced by a combination of both terms. Inertia terms of the fluid-dynamic forces were included in all cases. The mass ratio of the tubes for the calculations here is 100·0.

The results of the calculation for the square array are shown in Figure 9. As the figure shows, the critical velocity of damping-controlled instability is considerably greater than that of stiffness controlled instability. This means that the stiffness forces can supply more energy to induce instability than the damping force. The critical velocity of the combined instability is nearly equal to that of stiffness controlled instability. In this case, the damping force is added to the stiffness-controlled instability. The fluid-dynamic force c_{xox} has a positive phase difference as shown in Table 1, so the vibration in the x-direction is increased, but the vibration in the y-direction is suppressed because of the positive phase deference of c_{yoy}. This may be the reason why the critical velocities of stiffness-controlled instability and combined-controlled instability are almost at an equal level. By comparing with experimental results, it is understandable that the combined model is the best.

The results of a single row of tubes are shown in Figure 10. When using the damping term only, the critical velocity exists only in the low damping range. In the case of the stiffness term only, the line of critical velocity continues, while the critical velocity of combined instability becomes separated. The phase difference of c_{xox} on single row tubes is positive in the reduced velocity range of 2·2–8·0, while the phase difference of c_{yoy} positive is everywhere (see Table 2). So, as Figure 10 shows, the damping-controlled instability occurs in the reduced velocity range of about 2·2–8·0. The line of stiffness-controlled instability, however, continues everywhere. In the case of combined instability, the damping force in the low reduced-velocity range assists the vibration, but it suppresses the vibration in the high reduced-velocity range. The suppression effect in the reduced-velocity range of 10–20 is so

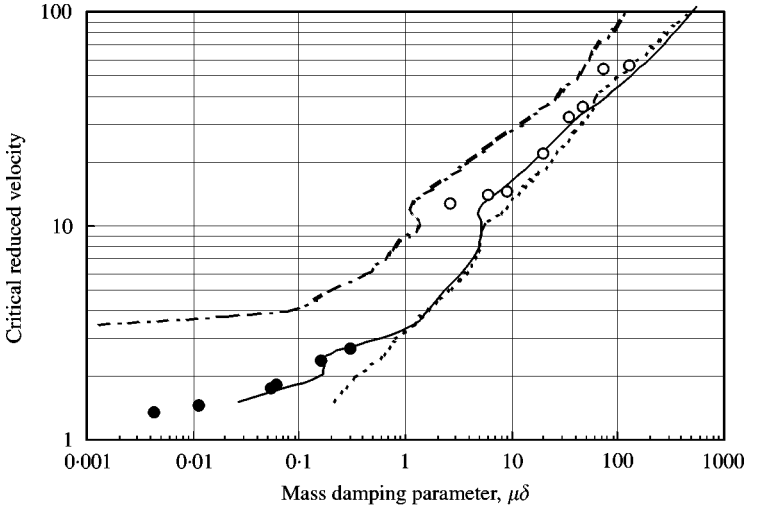

Figure 9. Critical velocities calculated by three methods (square tube array with $\mu = 100$): —— - —— - -, fluid-dynamic forces with damping terms only; - - - -, fluid-forces with stiffness terms only; ———, fluid-dynamic forces with both stiffness and damping terms; ○, experiments in air; ●, experiments in water.

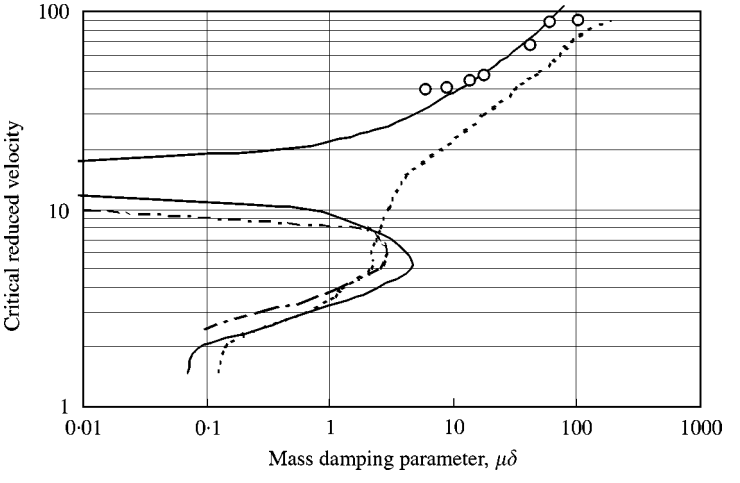

Figure 10. Critical velocities calculated by three methods (a single row of tubes with $\mu = 100$): — - — - -, fluid-dynamic forces with damping terms only; - - - -, fluid-forces with stiffness terms only; ———, fluid-dynamic forces with both stiffness and damping terms; ○, experiments in air.

great that the combined instability line is divided into two parts. The experimental results show that the combined model is the best.

4.3. Effect of Frequency Deviation

The natural frequencies of tubes in real plants display a considerable degree of scatter, because of production errors, or for design purposes. In the case of U-tubes, for example, each tube has an individual natural frequency. So, here the effect of frequency deviations was examined. The model tube bundle used in the calculation is one of four rows and three

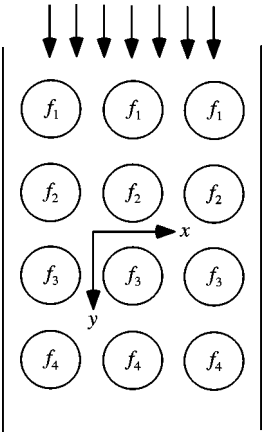

Figure 11. Tube arrangement used for frequency deviation calculation.

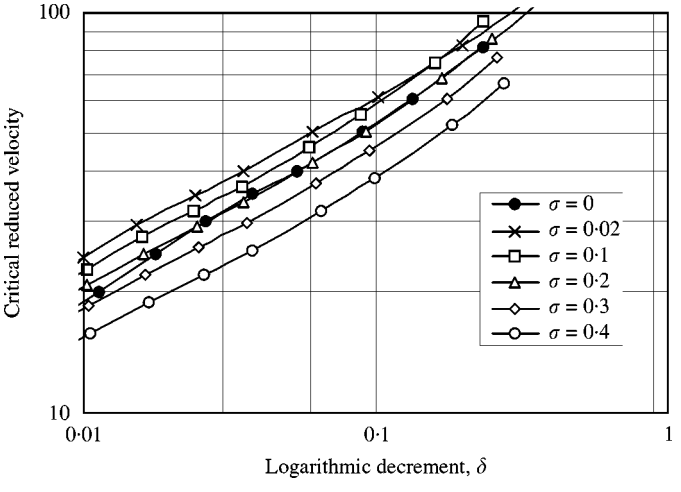

Figure 12. Critical velocity of tube array having different natural frequencies, Case A ($f_y = f_x$ for the array of Figure 11): σ, frequency deviation ratio.

columns, as shown in Figure 11. The mass ratio of the tubes is 1481·5. It is assumed that each tube has a different natural frequency in the x-direction (perpendicular to the flow), but the mean value of the frequencies is unity. The calculations were carried out by changing the frequency-deviation-ratio, which is defined as follows:

$$\sigma = \sum_{i=1}^{4} \frac{|f_m - f_i|}{f_m}, \quad \text{where } f_m = \frac{f_1 + f_2 + f_3 + f_4}{4} = 1{\cdot}0.$$

The tube in the first row has the highest natural frequency and that in the last row has the lowest frequency. There are two cases of frequency difference: in Case A, the natural frequency in the y-direction is the same as that in the x-direction ($f_y = f_x$), and in Case B, the natural frequency in the y-direction is twice of that in the x-direction ($f_y = 2f_x$).

The calculated critical reduced velocities are shown in Figures 12 (Case A) and 13 (Case B). The critical velocity of the tube bundle having a small frequency deviation is a little

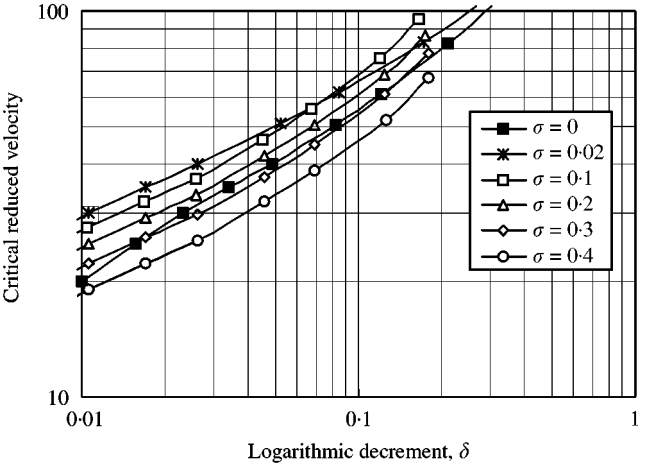

Figure 13. Critical velocity of tube array having different natural frequencies, case B ($f_y = 2f_x$ for the array of Figure 11): σ, frequency deviation ratio.

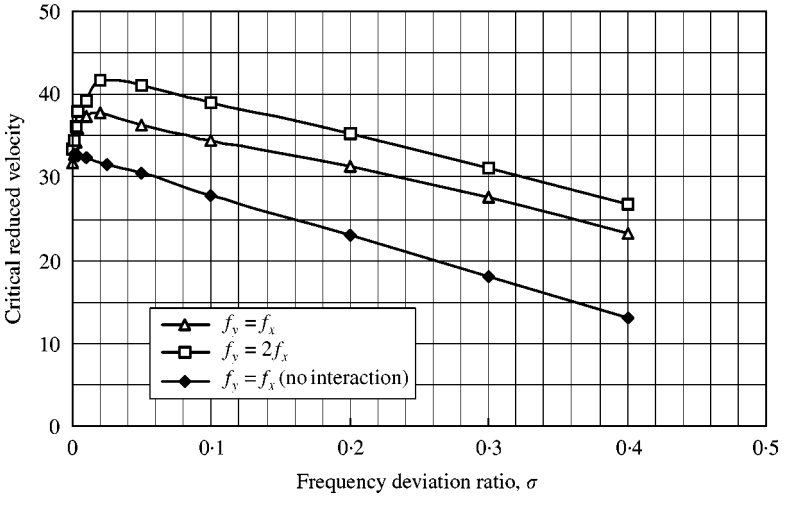

Figure 14. Effect of frequency deviation ratios on critical flow: △, $f_y = f_x$ for the array of Figure 11; □, $f_y = 2f_x$ for the array of Figure 11; ◆, no interaction between tubes.

larger than that of uniform frequency. However, when the deviation is larger than 0·2, the critical velocity decreases, because the natural frequency of the tube in the last row becomes small. The natural frequency in the y-direction in Case B is twice that of Case A. However, the critical velocity in Case B is only a little larger than that of Case A. Therefore, the vibration mode in the x-direction plays a more important role in the tube vibration.

The critical velocities versus frequency deviation are shown in Figure 14, where the logarithmic decrement is 0·03. In Case A, where the frequencies of x- and y-directions are the same, the maximum critical velocity occurs at a deviation ratio of about 0·02 and is about 20% larger than that for no frequency deviation. In Case B, the maximum velocity is for a deviation ratio of about 0·02 and is 25% larger. In all cases, the most susceptible tube is in the last row with the least natural frequency. If there is no interaction of vibration with

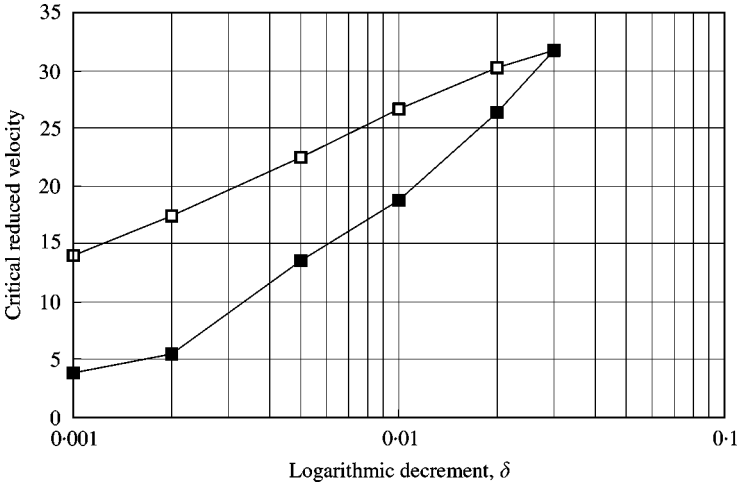

Figure 15. Effect of damping deviation on critical flow velocity: □, logarithmic decrement of the reference tube is changed while others are fixed at 0·03; ■, logarithmic decrement of all tubes are changed.

surrounding tubes, the critical reduced vibration must be proportional to the least natural frequency of the last row. Assuming that all the frequencies of all the tubes are equal to the least frequency in the last row, the critical velocities were calculated and the results are shown in Figure 14. The critical velocity for no frequency deviation is considerably smaller than the other velocities. From these results, it is reasonable to conclude that frequency deviation prevents orderly interaction among tubes and makes the critical velocity larger.

4.4. Effect of Damping Deviation

The logarithmic decrements of individual tubes are very different in real heat exchangers. The effect of deviations in the logarithmic decrement have also been examined. The mass ratio for these calculations is 1481·5. The logarithmic decrement of all tubes is fixed at 0·03, except for the reference tube that is in the second row of the second column in Figure 11. The logarithmic decrement of the reference tube was changed from 0·001 to 0·03. The calculated critical flow velocities are shown in Figure 15 as a function of the logarithmic decrement of the reference tube. The critical velocity gradually decreases with decreasing damping of the reference tube. The critical velocity of a tube bundle in which all tubes have a logarithmic decrement equal to that of the reference tube is also shown in the Figure 15 as solid square points. The vibration of the reference tube that has a small logarithmic decrement interacts with the surrounding tubes that have a larger one and, as a result, the critical velocity becomes larger.

4.5. Discussion

A tube bundle has many vibration modes. A sample of the vibration mode at a reduced velocity of 30·0 is shown in Figure 16(a). The tube bundle has equal frequencies and equal logarithmic decrement for each tube. The tubes interact with each other, such as to make the easiest mode to vibrate. Considering these effects, it can be said that the coupling mode has a very important role in tube bundle vibration. The stiffness terms make a vibration mode conducive to vibration and the damping terms work on this mode, so that the stiffness term and damping term work to mutually assist each other.

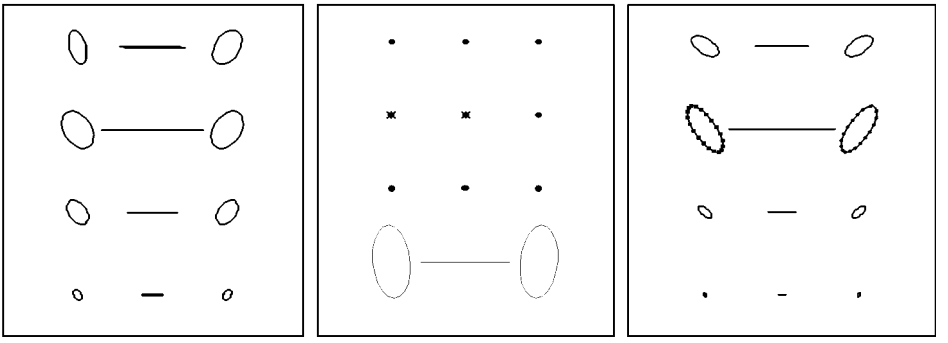

Figure 16. Vibration mode of tubes (reduced velocity = 30·0 for the array of Figure 11): (a) uniform natural frequency and uniform logarithmic decrement; (b) frequency deviation is 0·2 and logarithmic decrements are equal; (c) frequency is equal and logarithmic decrement of a tube with second row of second column is 0·01, while others are 0·03.

A deviation in natural frequency makes the critical velocity large, because the discrepancy of the frequency makes coupling difficult. The vibration mode of tubes having a frequency deviation of 0·2 is shown in Figure 16(b). The modal coupling between rows is interrupted. This interruption makes the critical velocity high, but if the deviation is very large, the critical velocity decreases because the smallest natural frequency in the last row becomes very small. The deviation of damping makes the critical velocity small because the small damping reduces the velocity. However, this characteristic is not very strong. The vibration mode of tubes, where the damping of the tube in the second row of the second column is 0·01 and the others are 0·03, are shown in Figure 16(c). The amplitudes of vibration in the second row become larger as compared to the case of equal logarithmic decrement. The change in vibration mode shows that the interaction of the vibration distributes the energy and shares it with the other tubes.

5. CONCLUDING REMARKS

Tube bundle vibration has usually many degrees of freedom and many different structural characteristics. Fluid-dynamic forces are affected by the vibration of each tube. Hence, we can talk about mutually excited vibration of each tube. The critical flow velocities of a tube bundle with various structural constraints were calculated and compared with the experimental data. The experimental data have been found to be in good agreement with the calculations, except for a few points, but the vibration characteristics were the same. So, further studies of vibration can be made using these fluid-dynamic forces.

The mass ratio and logarithmic decrement must generally be used separately. The frequency of a tube is changed with the fluid-dynamic force and, in the case of small mass ratio, the effect is very large. In the case of a mass ratio larger than 10, the frequency is not changed drastically. So, the mass-damping parameter is applicable in the mass-ratio range larger than 10. However, the frequency changes significantly in the range less than 10; therefore, the mass ratio and logarithmic decrement must be used separately.

Summarizing the results, the following itemized conclusions may be made.

1. If the mass ratio is larger than 10, the critical velocity can be expressed as a function of the mass-damping parameter. However, when the mass-ratio is less than 10, the mass ratio and the logarithmic decrement must be used separately.

2. Stiffness terms and damping terms in the fluid-dynamic forces assist each other. So, the vibration must be considered as a combined instability, i.e. neither purely damping-controlled nor purely stiffness-controlled.

3. When the deviation in frequency between the tubes is small, the critical velocity increases. If the deviation is large, the velocity decreases because the smallest natural frequency of the system becomes small; but the rate of decrease is slow.

4. The deviation in damping between tubes makes the critical velocity larger because the interaction of the vibration distributes the energy and shares it with other tubes.

In these calculations, the coupled set of differential equations of each tube has been used, so the effects of different structural characteristics of each tube can be taken into account. The unsteady fluid-dynamic forces at each reduced velocity are shown in Tables 1 and 2. We expect that the calculation method and the fluid-dynamic force data will be widely used.

References

CHEN, S. S. 1983 Instability mechanisms and stability criteria of a group of circular cylinders subjected to cross-flow. Part 1: Theory; Part 2: Numerical results and discussions. *ASME Journal of Vibration, Stress and Reliability in Design* **105,** 51–58 and 253–260.

CHEN, S. S., CAI, Y. & SRIKANTIAH, G. Y. 1998 Fluid damping controlled instability of tubes in cross flow. *Journal of Sound and Vibration* **217,** 883–907.

PAIDOUSSIS, M. P. 1983 A review of flow-induced vibrations in reactor and reactor components. *Nuclear Engineering and Design* **74,** 31–60.

PRICE, S. F. 1995 A review of theoretical models for fluid-elastic instability of cylinder arrays in cross-flow. *Journal of Fluids and Structures* **9,** 463–518.

TANAKA, H. & TAKAHARA, S 1980 Unsteady fluid-dynamic force on tube bundle and its dynamic effect on vibration. In *Flow Induced Vibration of Power Plant Components* (ed. M. K. Au-Yang), pp. 77–92, ASME PVP-41. New York: ASME.

TANAKA, H. & TAKAHARA, S. 1981 Fluid elastic vibration of tube array in cross flow. *Journal of Sound and Vibration* **77,** 19–37.

WEAVER, D. S. & FIZTPATRICK, J. A. 1988 A review of cross-flow induced vibrations in heat exchanger tube arrays. *Journal of Fluids and Structures* **2,** 73–93.

APPENDIX A: NOMENCLATURE

C	equivalent fluid-dynamic coefficient
c	fluid-dynamic coefficient
D	damping coefficient
d	tube diameter (m)
F	fluid-dynamic force (N)
k	stiffness coefficient
m	tube mass of unit length (kg/m)
t	time (s)
U	gap velocity between tubes (m/s)
V_r	reduced velocity, $V_r = 2\pi U/d\omega$
X, Y	displacement in the x- and y-direction (m)
x, y	coordinate of tube vibration
z	coordinate of cylinder axis
δ	logarithmic decrement
δ_c	critical logarithmic decrement
δ_{ij}	Kronecker's delta
η	flow distribution along z-axis (m/s)
λ	eigenvalue

μ mass ratio, $\mu = m/\rho d^2$
$\mu\delta$ mass-damping parameter
ξ vibration mode of tube along z-axis
ρ density of fluid (kg/m^3)
φ phase difference between tube vibration and fluid-dynamic force
Ω frequency ratio
ω angular frequency (rad/s)
ω_o reference angular frequency (rad/s)